Journal of Membrane Science 474 (2015) 114–121

Contents lists available at ScienceDirect

Journal of Membrane Science

journal homepage: www.elsevier.com/locate/memsci

Preparation and characterization of carbon and carbon/zeolite membranes from ODPA–ODA type polyetherimide

Bing Zhang [a,b,*], Yonghong Wu [a], Yunhua Lu [b,c], Tonghua Wang [b], Xigao Jian [b], Jieshan Qiu [b,1]

[a] School of Petrochemical Engineering, Shenyang University of Technology, Liaoyang 111003, China
[b] Carbon Research Laboratory, Liaoning Key Lab for Energy Materials and Chemical Engineering, State Key Lab of Fine Chemicals, School of Chemical Engineering, Dalian University of Technology, Dalian 116024, China
[c] School of Chemical Engineering, Liaoning University of Science and Technology, Anshan 114051, China

ARTICLE INFO

Article history:
Received 8 February 2014
Received in revised form
23 September 2014
Accepted 26 September 2014
Available online 7 October 2014

Keywords:
Polyetherimide
Carbon membranes
Zeolite
Gas permeation

ABSTRACT

A novel precursor, 3,3′,4,4′-oxydiphthalic dianhydride-4,4′-oxydianiline (ODPA–ODA) type polyetherimide (PEI), was synthesized and used to prepare carbon membranes by preoxidation and heat treatment. The thermal stability of the ODPA–ODA type PEI was evaluated by thermogravimetric analysis. The surface properties, elemental composition, microstructure, morphology and gas separation performance of the as-made carbon membranes were examined by the Fourier transform infrared spectroscopy, elemental analysis, X-ray diffraction, scanning electron microscopy and gas permeation techniques. The effects of the preoxidation temperature and zeolite incorporation on the microstructure and gas separation performance of carbon membranes were investigated. The results have shown that ODPA–ODA type PEI is a good precursor for producing carbon membranes. The preoxidation of the ODPA–ODA type PEI is essential to make defect-free carbon membranes, which also helps to improve the thermal stability and porosity during pyrolysis by forming crosslinking structure in precursor. The carbon membranes made after preoxidation at 480 °C and heat treatment at 650 °C have an oxygen permeability of 131.5 Barrer and an ideal O_2/N_2 selectivity of 9.7. The incorporation of ZSM-5 into the carbon membranes further helps to improve the separation performance of the carbon/zeolite membranes for H_2/N_2 gas mixture.

1. Introduction

Carbon molecular sieve membranes (CMSMs, or carbon membranes for short), a kind of porous inorganic membrane material with tuned pore structures, have drawn much attention since 1980s simply because they can efficiently separate gas mixtures via the molecular sieving mechanism [1]. The CMSMs have many unique properties such as chemical and thermal stability, and are of great potential in a variety of gas separation applications including the enrichment of nitrogen or oxygen from air, the separation of hydrogen from gasification gas, the purification of natural gas, the recovery of hydrogen from hydrocarbons, the separation of light alkenes/alkanes, the removal of organic vapor or sour gas from mixture, *etc.* [2]. Nevertheless, up to now, few CMSMs are available commercially though the Blue Membranes GmbH in Germany is producing plate-type CMSMs and the Carbon Membranes Ltd. in Israel is offering hollow fiber CMSMs on a pilot scale. The high production cost of the CMSMs is one of the key issues that has hindered their commercialization, and this is especially the case in comparison to the conventional polymeric membranes [3,4]. In general, the CMSMs can be made by the pyrolysis of polymeric membranes, and in this regard, considerable efforts have been made in terms of developing cheap precursors or optimizing preparation procedure with an aim of reducing the production cost of the CMSMs [2,5]. The precursor of the CMSMs plays a key role of governing both the production cost and the structure and gas separation performance of the CMSMs to a great degree [6]. Among the new precursors developed recently, the polyetherimide (PEI), a series of derivatives of polyimide with flexible C–O bonds in the molecular backbones, has attracted more attention. The PEI has aromatic imide units that result in stiffness and heat resistance, and the swivel groups such as –O– that function as flexible chains and result in good processability. These features endow the PEI with many advantages over the traditional polyimides, including good solubility and thermoplastics, low cost and easy processability. These make the PEI hold promise as a precursor for carbon membranes [6]. There are some reports about the preparation of

* Corresponding author at: Carbon Research Laboratory, Liaoning Key Lab for Energy Materials and Chemical Engineering, State Key Lab of Fine Chemicals, School of Chemical Engineering, Dalian University of Technology, Dalian 116024, China. Tel.: +86 419 5319450; fax: +86 419 5311989.
E-mail addresses: bzhangdut@163.com (B. Zhang), jqiu@dlut.edu.cn (J. Qiu).
[1] Tel.: +86 411 84986024; fax: +86 411 84986015.

http://dx.doi.org/10.1016/j.memsci.2014.09.054
0376-7388/

PEI-based carbon membranes. Fuertes and Centeno [7] prepared plate-like CMSMs from the PEI by pyrolysis at 800 °C, showing a selectivity for gas pairs O_2/N_2 of 7.4, He/N_2 of 121, CO_2/CH_4 of 25 and CO_2/N_2 of 15. Sedigh et al. [8] made tubular CMSMs from 1,4-bis (3,4-dicarboxyphenoxy)-benzene dianhydride type PEI by pyrolysis at 600 °C, showing a separation factor of 145 for CO_2/CH_4 and 155 for H_2/CH_4. They also fabricated Ultem 1000 type CMSMs from the PEI, showing a CO_2/CH_4 permselectivity of 12.5 [9]. Favvas et al. [10] obtained hollow fiber CMSMs from a blend of 3,3′4,4′-benzophenone tetracarboxylic dianhydride, 80% methylphenylene-diamine and 20% methylene diamine co-polyetherimide (P84) by pyrolysis at 900 °C, showing a separation factor of 843 for H_2/CH_4 at 100 °C. Nevertheless, the CMSMs mentioned above are not defect-free, and cannot meet the requirements for the separation of permanent gas mixtures, which may be due to the thermoplastic property of the PEI that undergoes a melting stage in the heat treatment step. It has been partly demonstrated that the cross-linking structure formed in a temperature range between the glass transition temperature (T_g) and degradation temperature (T_d) of the PEI helps to eliminate the melting stage, and to improve the separation performance of the final CMSMs [11,12]. The crosslinking of the thermoplastic polymeric PEI has resulted in the formation of oxygen bridges between the aromatic molecules, which helps to tune the growth of aromatic crystallites during the pyrolysis step by forming amorphous carbon structures. As such, the CMSMs with a tuned pore structure can be fabricated [13]. Hosseini and Chung [14] and Salleh and Ismail [15,16] have made PEI-based CMSMs by making use of p-xylene diamine as cross-linker and by air preoxidation before the pyrolysis step. Wey et al. [17] have made composite membranes by coating the crosslinked PEI on Al_2O_3 support at 240 °C for 6 h.

Herein, we report on the synthesis of a novel precursor, 3,3′, 4,4′-oxydiphthalic dianhydride-4,4′-oxydianiline (ODPA–ODA) type PEI, for the preparation of CMSMs. Fig. 1 shows the chemical structure and the schematic stereo-structure of the repeated basic unit in ODPA–ODA PEI molecules. Compared with the traditional PEI molecules, the ODPA–ODA PEI has a simple molecular structure, in which the flexible oxygen bridging units between the diphenyl linkages have changed the rigidity of the chain segments resulted from the bulky groups. This chemical structure helps to prevent the tight packing of the polymeric chains, and finally result in membrane materials with improved gas permeation properties [18,19]. Because of this unique chemical structure, the ODPA–ODA PEI has been tested for making separation membranes, and the insulator of microelectronic devices [20–23]. However, to our best knowledge, little has been done on the production of CMSMs from the ODPA–ODA PEI. In the present work, the ODPA–ODA PEI was used to make high performance CMSMs for gas separation. The variation of the structure and property of the PEI precursor and the as-made CMSMs have been investigated in terms of the influence of the preoxidation and pyrolysis conditions. Our previous work has demonstrated that the gas separation performance of the CMSMs can be efficiently tailored, to some degree, by incorporating porous inorganic additives such as zeolites into the membrane matrix [24,25]. With this in mind, here we also studied the influence of the added ZSM-5 on the separation performance of the carbon/zeolite membranes.

2. Experimental

2.1. Preparation of carbon membranes

A poly(amic acid) (PAA) solution of ODPA–ODA type PEI was first synthesized by a typical condensation polymerization reaction of two monomers, 3,3′,4, 4′-oxydiphthalic dianhydride and 4, 4′-oxydianiline in N-methyl-2-pyrrolidone (NMP). Before polymerization, the commercial monomers, ODPA and ODA, were purified by recrystallization in acetic anhydride and tetrahydrofuran, respectively. Then, they were dried at 140 °C under vacuum. The NMP was distilled over CaH_2 before use. The polymerization reaction was conducted at room temperature with an equimolar amount of ODPA and ODA in an appropriate amount of NMP under constant stirring and in flowing N_2 for 6 h. Finally, a transparent homogeneous PAA solution was obtained with a solid content of *ca.* 15 wt%.

Free-standing polymeric membranes were fabricated by a casting method in a dust-free environment. First, the pre-polymer PAA solution was directly casted onto clean glass plates to make polymeric membranes, which were dried at 40, 60, 100 and 200 °C for 24 h, in order to completely remove the remaining solvent and to make stable imidization moieties with tuned molecular structure. The as-made PEI membranes were cut into coin-like sheets with a diameter of *ca.* 3.2 cm before the subsequent heat treatment. In order to avoid or eliminate the melting stage in the pyrolysis step, the PEI membranes were preoxidized in air at a rate of 2 °C/min from room temperature to a pre-set temperature for 30 min. Then, the preoxidized membranes were heated in a horizontal tubular furnace, first at a heating rate of 2 °C/min from room temperature to 200 °C for 30 min, then to 300 °C for 30 min, and 400 °C for 30 min, and during this period, the imidization of molecules was fully completed. Then, the membranes were further

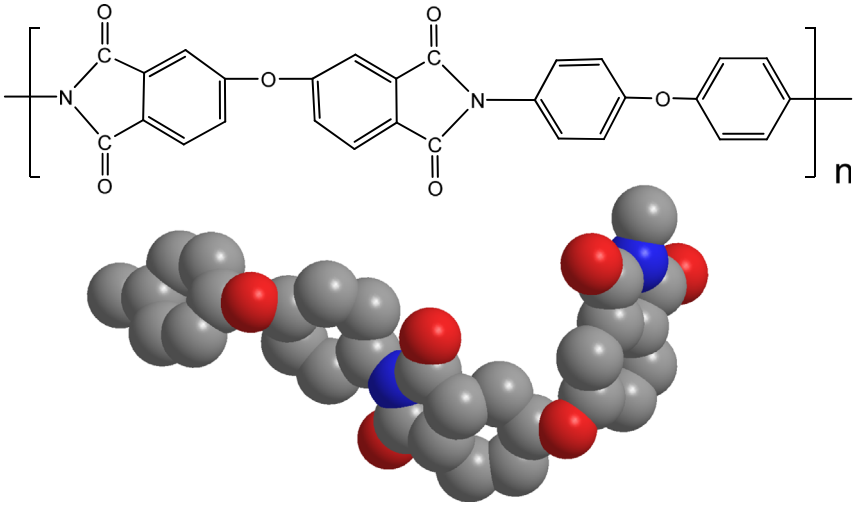

Fig. 1. Chemical structure of repeated unit in ODPA–ODA type Polyetherimide.

heated to 650 °C at 1 °C/min for 60 min, yielding the CMSMs after the furnace being naturally cooled down back to room temperature.

The ZSM-5 composite CMSMs were also fabricated by the procedure described above. The ZSM-5 type zeolite with a mean particle size of 1.25 μm was used. ZSM-5 with a ratio of 0.5 wt% in the whole solution was added into the prepolymer solution under vigorous stirring and ultrasonic conditions for 30 min. The as-made PEI membranes, ZSM-5/PEI membranes, preoxidized membranes, CMSMs and ZSM-5 composite CMSMs were denoted as PEI, PZM, OM-*t*, CM and CZ, respectively. Here, the letter "*t*" in OM-*t* refers to the preoxidation temperature.

2.2. Characterization

The membranes were examined by a Nexus 470 ATR-Fourier Transform Infrared (FTIR) spectroscopy (Thermo Nicolet, with OMNIC software) in a wavenumber range of 4000–680 cm^{-1} to analyze the functional groups.

The elemental compositions of the membranes were analyzed by Euro EA-3000 elemental analyzer (Leeman Labs Inc., USA). For comparison, all the element moles of the membranes were normalized with the molar quantity of nitrogen in the PEI as reference.

The carbon structure of membranes was analyzed by a D/max2500 model X-ray diffraction analyzer (Rigaku, operated at 40 kV and 80 mA) in a 2θ range of 5–60°. The microstructure of the preoxidized samples was analyzed by a Shimadzu X-ray diffractometer XRD-7000 operated at 40 kV and 30 mA.

The thermo-gravimetric analysis of the PEI precursors was carried out by a Diamond TG-DTA6300 model TG analyzer (Perkin Elmer, USA) at a heating rate of 10 °C/min from room temperature to 900 °C in flowing nitrogen.

The average particle size of zeolite ZSM-5 was analyzed by a DLS particle size analyzer (Model: ZEN3690, Malvern Instruments Ltd., UK).

The surface morphology and microstructure of the membranes were examined by a TM-3000 scanning electron microscopy (Hitachi) at accelerating voltage of 15 kV.

The adsorption isotherms of the membranes were recorded at −196 °C by an ASAP 2420 nitrogen adsorption analyzer (Micromeritics, USA), and the pore size distribution of micropores was calculated by the Horvath–Kawazoe (HK) method.

Single gas permeation of the membranes was tested by traditional variable volume–constant pressure method using high purity gases (≥ 99.999%), *i.e.*, H_2, CO_2, O_2, and N_2. The permeation of mixture gas (O_2/N_2 with a volume ratio of 21/79) was also tested to evaluate the practical gas separation performance of the membranes. The mixed gas flowed across the upper side of the membrane at a rate of 4 mL/min, at the same time, the carrier gas (Argon) sweeping on the permeation side at a rate of 2 mL/min to direct the permeated gas to gas chromatography (GC) for analysis. The GC analysis was conducted by GC 7890 (Techcomp LTD.) equipped with a thermal conductivity detector (TCD) and a packed column (5A molecular sieve 2 m × 2 mm I.D. column). For each membrane, the measurements were undertaken for more than three samples prepared under the same conditions. The reported permeation data are the averaged value with a measurement precision of 10%. For the details of the test procedure, please refer to our previous report [26].

3. Results and discussion

3.1. The effect of preoxidation

High performance CMSMs need to have good integrity and well-tuned porous structure and to be free of defects. It has been found that the preoxidation treatment before the pyrolysis of the ODPA–ODA type PEI can effectively avoid the melting stage that may result in poor integrity and pore structure of the CMSMs. In order to produce defect-free CMSMs from ODPA–ODA PEI, the preoxidation conditions have been addressed in detail in terms of chemical properties and microstructure of the ODPA–ODA PEI.

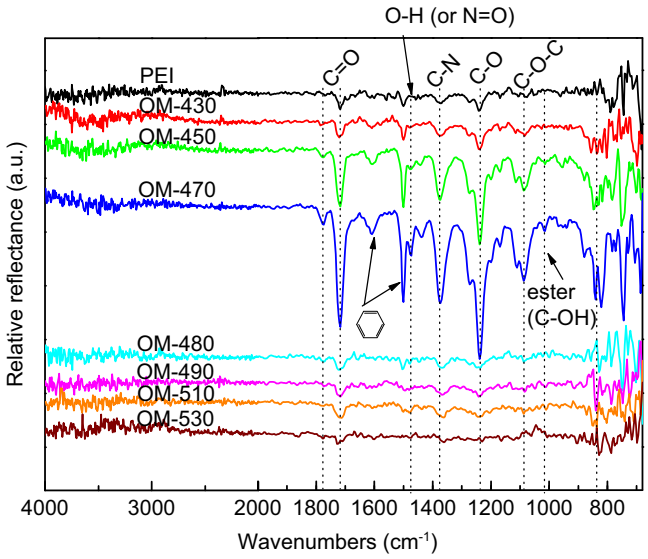

Fig. 2. ATR-FTIR spectra of samples preoxidized at different temperatures.

3.1.1. Functional groups

Fig. 2 shows the FTIR spectra of the starting and preoxidized PEIs. In the case of starting PEI, typical reflectance bands related to the imide structure can be clearly seen at 1782, 1720, 1377, and 747 cm^{-1}, which are due to the symmetric and asymmetric coupling vibrations of the carbonyl groups in imide rings, the stretching vibration of C–N bond and imide rings or imide type carbonyl. The bands at 1605 and 1500 cm^{-1} are due to the skeleton vibration of the benzene ring. The bands at 1239 and 1086 cm^{-1} are due to the asymmetrical stretching vibration of C–O bonds and C–O–C groups. The spectra have evidenced the existence of typical imide groups and other functional groups in the molecular structure of ODPA–ODA type PEI, as shown in Fig. 1.

For the preoxidized membranes, two bands related to the C–NH group at 1550 cm^{-1} and CONH group at 1665 cm^{-1} have disappeared. This means that the poly(amic acid) groups have been completely converted to imide groups after the preoxidation treatment. At the same time, the band intensity for the imide groups increases markedly as the preoxidation temperature increases from 430 to 470 °C, meanwhile, the membrane color gradually turns from transparent light yellow to opaque dark. In addition, the hydrogen substitution of aromatic benzene rings has become more obvious below 900 cm^{-1} after the preoxidation treatment. And two new bands at 1017 and 1477 cm^{-1} can be observed for the preoxidized membranes, which are due to aromatic or aliphatic ester bonds or C–OH stretching vibration and O–H in-plane deformation or N=O stretching vibration. This has confirmed the formation of crosslinked structure in the inter- and intra-molecules by oxygen bridges via the ester or ether groups.

It can also be seen that the band intensity drops as the temperature is further increased from 480 to 530 °C. This might be due to some other reactions such as the thermal decomposition, recombination or reorganization, which are in parallel to the crosslinking reactions. At higher temperatures, the thermal decomposition reactions would be dominant. By comparing the

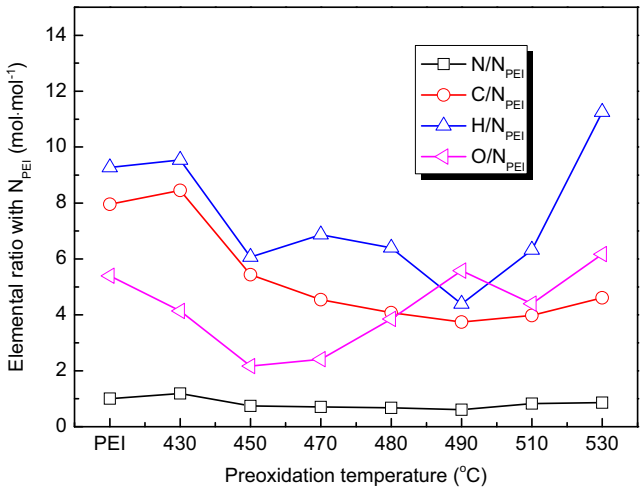

Fig. 3. Evolution of element compositions in membrane samples with varying preoxidation temperatures.

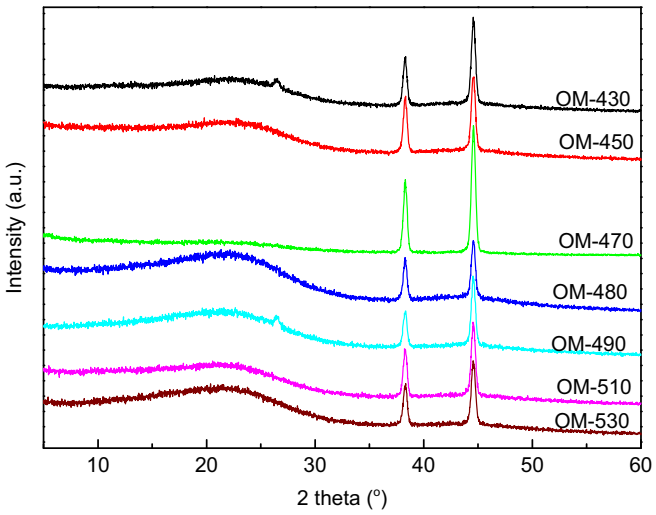

Fig. 4. XRD patterns of preoxidized membranes prepared at different temperatures.

different changes in the band intensity in the two temperature ranges, one can envision that the crosslinked structure is continuously constructed before 470 °C, and a turning point for the microstructure appears at the temperature over 480 °C. The microstructure of the OM-480 membrane starts to collapse significantly after the air oxidation. As the preoxidation temperature increases from 480 to 530 °C, the intensity of all bands decreases further or some bands even disappears completely, implying strong thermal degradation or oxidation of the crosslinked structure [27,28]. With this formation in mind, the suitable preoxidation temperature should be 470 or 480 °C, at which both the formation and the oxidation of the crosslinked structure can be balanced to some degree.

3.1.2. Elemental composition

Fig. 3 shows the relative compositions of four elements, *i.e.*, C, H, O and N, in membranes made after the preoxidation at different temperatures. The values vary in an order of H > C > O > N. The H content tends to drop as the preoxidation temperature increases from 430 to 490 °C. The N content fluctuates slightly in the whole temperature range. The change of the O content is quite different from other elements. It goes to a minimum value at 450 °C, and then rises to a maximum value at 490 °C. The increment of the O content as the temperature increases from 450 to 490 °C is probably due to the formation of oxygen-containing crosslinked structure resulted from the introduction of free oxygen radicals in the air oxidation step [12]. When the preoxidation temperature is over 490 °C, the thermal degradation and excessive oxidization reactions would take place, leading to the breakage of crosslinked structure [11]. Because of this, both the O and C content drop, as shown in Fig. 3. This result is in good agreement with the FTIR results discussed above.

3.1.3. Microstructure

Fig. 4 shows the XRD patterns of the preoxidized membranes, showing typical broad peaks at *ca.* 23° due to the (002) plane diffraction of amorphous structure, and the strong peaks at *ca.* 44° due to the (100) plane diffraction [26]. The interlayer distance parameters, d_{002} and d_{100}, were calculated by Bragg's equation. As plotted in Fig. 5, the d_{002} value of the preoxidized membranes goes up first then drops as the temperature increases, and a maximum value of 0.413 nm is obtained at 510 °C. The variation tendency of the d_{100} value is very similar to that of the d_{002} value except for the maximum value at 490 °C. As the preoxidation temperature increases, the interlayer distance increases first, which is due to

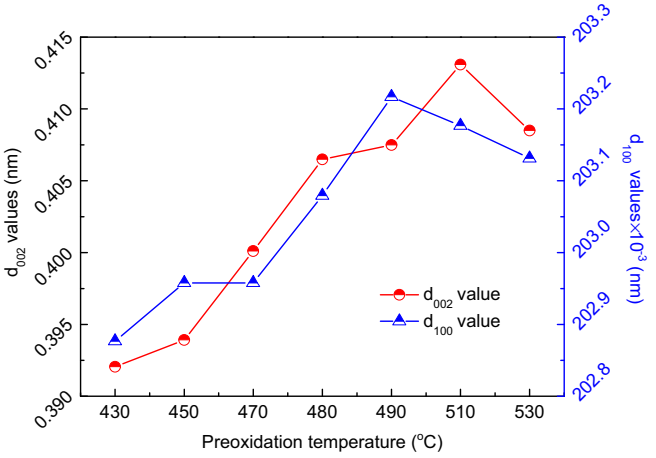

Fig. 5. Effects of preoxidation temperature on structural parameters in membrane samples.

the successive construction and expansion of crosslinked networks in microstructure [29]. When the preoxidation temperature is over 490 °C, some structures in the pre-organized crosslinking network would collapse due to the thermal degradation and excessive oxidation reactions, leading to the decreased interlayer distance. This trend is in good agreement with the results of elemental and FTIR results discussed above.

In order to quantitatively determine the crosslinking extent of the membranes, a dissolution test was conducted by dissolving the preoxidized membranes in NMP at 50 °C for 24 h [27,30]. The percentage of the insoluble composition is 98.71% for OM-430, 98.76% for OM-450, 98.77% for OM-470, 98.88% for OM-490, 99.51% for OM-510 and 99.71% for OM-530. This implies that the crosslinking degree of the membranes increases monotonously as the preoxidation temperature increases from 430 to 530 °C. Nevertheless, it should be noted that the percentage of the insoluble composition cannot fully represent the crosslinking degree when the preoxidation temperature is over T_d (*e.g.*, 490 °C) because of the damage in the crosslinked structure by the thermal degradation and excessive oxidation [31,32]. As such, the preoxidation at higher temperature alone cannot ensure the production of defect-free carbon membranes.

After taking into account of various factors including the membrane integrity, the degree of oxidation and thermal degradation, a temperature of 480 °C for the preoxidation was assumed to be

optimal to make carbon membranes with excellent performance under the conditions adopted in the present study.

3.1.4. The preoxidation mechanism

The results presented above may lead one to believe that the formation of crosslinked structure for the ODPA–ODA PEI in the preoxidation step has taken place. Three kinds of reactions may be involved in the air oxidation of PEI: oxidation, dehydrogenation and crosslinking [28]. The first two reactions are very important to induce the occurrence of crosslinking. The oxidation reaction is initiated by the attacking of oxygen to the main chain of the PEI molecule, resulting in the cleverage of molecular chains and the formation of oxygen-containing functional groups [33,34]. The dehydrogenation reaction is accompanied in the conversion of C–C bonds to C=C bonds in the molecular chains in the presence of active oxygen species, yielding oxygen-containing groups such as –OH and C=O [6,35]. With the oxygen-containing groups from the above two reactions, crosslinked network structures that are thermally stable would be formed in inter- and intra-molecular chains due to the coalescent reactions by hydrogen bonds, ether bonds, and ester bonds [33]. The crosslinking structure is most favorable for the preparation of CMSMs from PEI, confirmed by the fact that the melting stage and the excessive removal of carbon element in the pyrolysis step have been avoided.

3.2. Thermal stability of PEI precursors

The thermal stability of the PEI precursors was examined, and the curves of the thermal degradation and the weight loss rate for PEI, OM-480 and PZM are presented in Fig. 6. At temperatures below 200 °C, the minor weight loss for the PEI is due to the evaporation of residual solvent NMP (b.p. 202 °C). For the PEI, a striking thermal degradation stage appears at 200–350 °C owing to the removal of a large amount of water resulted from the thermal imidization reaction [36]. At temperature over 500 °C, a major thermal weight loss period for the PEI appears at 570 °C with a rate of 249.7 μg/min. In comparison to the PEI, the weight loss for PZM is smaller in the first two stages (< 200 °C, 200–350 °C). At the same time, the major thermal degradation stage has shifted 5 °C to higher temperatures, with a rate of 160 μg/min. This has evidenced that the addition of ZSM-5 zeolites helps to improve the thermal stability of the membranes. However, the addition of ZSM-5 in the membrane matrix does not obviously affect the final char yield, evidenced by the fact that both PEI and PZM have a similar yield of *ca.* 55.5 wt%. In the case of the preoxidized membranes, the OM-480 has a thermal degradation profile similar to that of PEI and PZM, except for a much higher peak at 590 °C. At the final temperature of 900 °C, the yield of OM-480 is 62.2%, which is significantly higher than the other two samples. This further shows that the preoxidation can substantially improve the thermal stability of the PEI membranes.

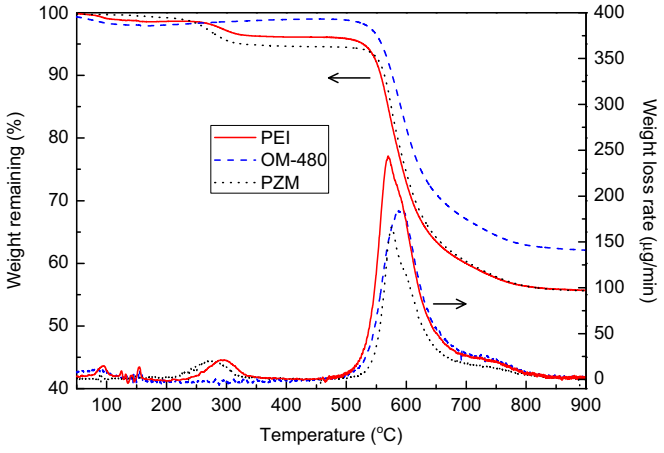

Fig. 6. The curves of thermal degradation and weight loss rate for precursors.

3.3. Morphology of carbon membranes

Fig. 7 shows the SEM images of CM and CZ membranes, showing a smooth surface of the concerned membranes. No defects or cracks can be observed on the membrane surface. For the CZ membrane, the zeolite particles are uniformly dispersed on the surface and cross-section of the membrane without any lumpy aggregations. The thickness for CM membrane is 78.4 μm, and it is 89.2 μm for the CZ membrane. The microstructure including the carbon structure and pore structure, and the gas permeation of these membranes will be discussed below.

3.4. Microstructure of carbon membranes

The XRD technique has been widely used to analyze the microstructure of materials. As shown in Fig. 8(a), the original PEI membrane has a relatively symmetric and broad diffraction peak at 17.7° due to the (002) plane diffraction. Whereas, the peak position of (002) plane diffraction shifts to 20.5° for OM-480 and 21.4° for CM. Simultaneously, the peak of (002) plane diffraction becomes more asymmetrical. The change in the XRD patterns implies that the original ordered microstructure of polymer PEI has collapsed, and been reorganized by forming a cross-linked network structure after the preoxidation treatment, and an amorphous carbon structure is finally formed after the pyrolysis [6]. According to Bragg's equation, the d_{002} value of the OM-480 is 0.43 nm, and it is 0.41 nm for the CM. A similar variation trend of the d_{002} value was also observed for carbon membranes made from thermoplastic poly(phthalazinone ether sulfone ketone) reported previously [13]. This means that the interlayer distance becomes smaller, and the microstructure becomes more compact after the pyrolysis. In Fig. 8(b), the diffraction peaks of ZSM-5 can be seen at 7.7, 8.8, 23.1, 23.9, 30.0 and 45.0° [37]. However, for the CZ membranes, the weak diffraction peaks of ZSM-5 are overlapped by the two big characteristic diffraction peaks of (002) plane at 23.3° and (100) plane at 44.5° for carbon materials. The structure of the CZ membranes is looser than that of the CM because its (002) plane diffraction angle is lower by 1.9°. To further clarify this, the microporous structure of the carbon membranes is analyzed below.

3.5. Microporous structure of carbon membranes

The N_2 adsorption isotherms, and the micropore size distribution of carbon membranes, are shown in Fig. 9. The N_2 adsorption capacity of the CZ membrane is 3 times higher in magnitude than that of the CM at the final relative pressure. This implies that the addition of ZSM-5 has significantly boosted the micropore volume in the carbon membrane matrix, which increases from 0.064 $cm^3\,g^{-1}$ for the CM to 0.221 $cm^3\,g^{-1}$ for the CZ. At the same time, the average pore size of the membranes drops slightly from 6.0 Å for the CM to 5.7 Å for the CZ, which is due to the incorporation of ZSM-5 with a microporous channel of *ca.* 5–5.5 Å in diameter. The inset of Fig. 9 shows the micropore size distribution curves, demonstrating the contribution of ZSM-5. Obviously, the porous structure of carbon membranes can be effectively adjusted by incorporating the ZSM-5 particles into the carbon matrix, which helps to further modify the gas separation performance of the carbon membranes [38].

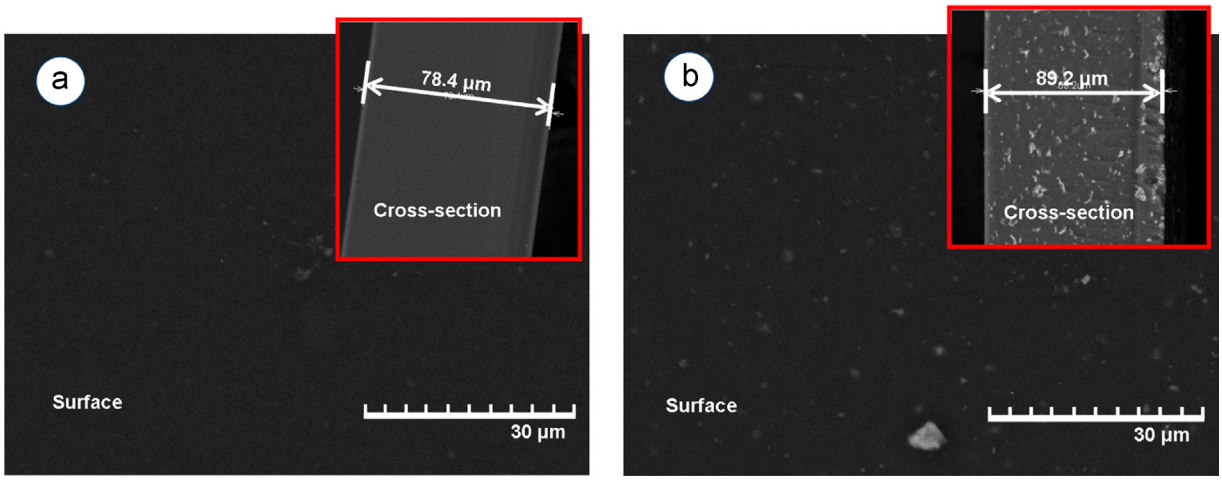

Fig. 7. SEM images of (a) carbon membranes, and (b) carbon/ZSM-5 membranes.

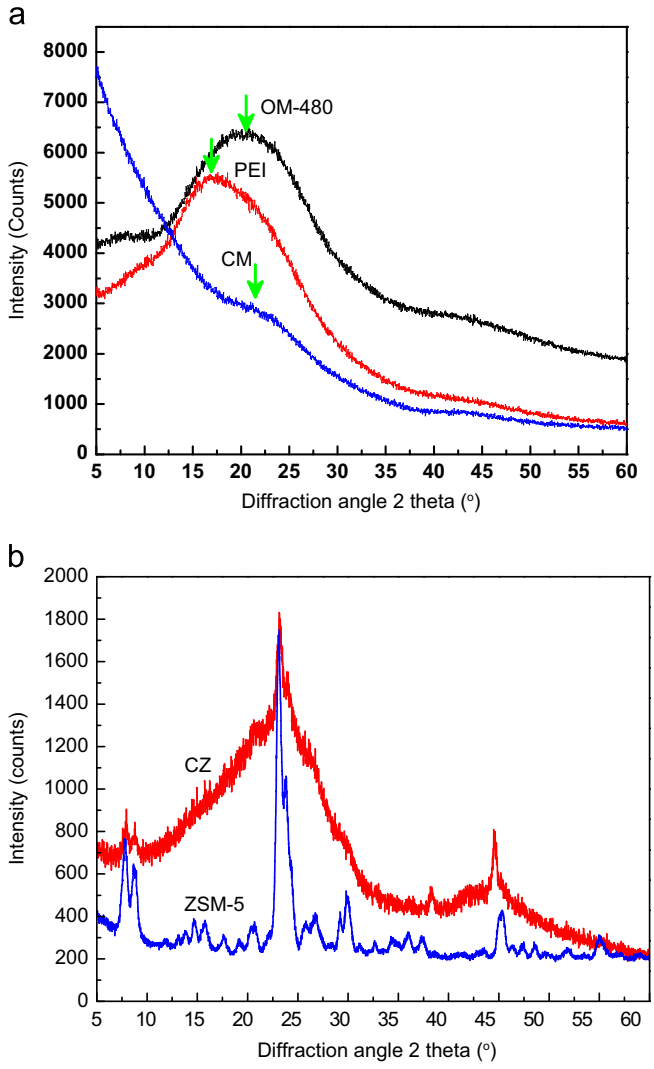

Fig. 8. XRD patterns of samples. (a) Evolution from polymeric membranes to carbon membranes, (b) ZSM-5 and its composite carbon membranes.

3.6. Gas permeance of carbon membranes

Table 1 shows the gas permeation data of the carbon membranes, showing that the permeabilities of the four single gases for all carbon membranes are exactly in the reverse order of their kinetic diameters (H_2, 0.289 nm; CO_2, 0.33 nm; O_2, 0.346 nm; and N_2, 0.364 nm). This implies that the dominant mechanism involved in the permeation of gases through the CMSMs is the molecular sieving one. In addition, the permeabilities of the CMSMs increase as the permeation temperature increases from 50 to 90 °C, suggesting that the gas permeation through the CMSMs is a temperature-activation process. Based on Eq. (1) that is the natural logarithmic form of the Arrhenius equation, four linear fitting curves can be plotted as the logarithmic permeability *vs.* the reciprocal Kelvin temperature, with a mean square deviation of 0.98. From the slope of the four lines, the activation energy for the gas permeation can be determined, and it is 4.46 kJ/mol for H_2, 5.97 kJ/mol for CO_2, 15.27 kJ/mol for O_2 and 3.48 kJ/mol for N_2. These values are comparable to those reported in the literature [39,40]. Due to fact that the activation energy of H_2, CO_2 and O_2 is higher than that of N_2, the selectivity of the CMSMs is improved as the permeation temperature increases, as shown in Table 1.

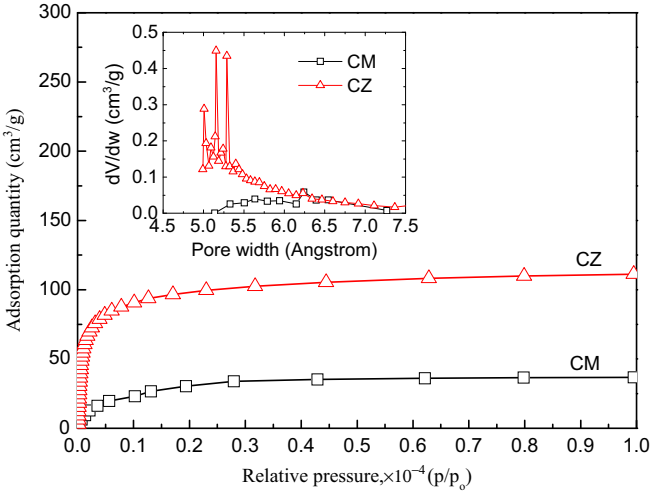

Fig. 9. Adsorption isotherms and micropore size distribution curves.

$$\ln P = \ln P_0 - \frac{E_a}{RT} \quad (1)$$

where, P, P_0, E_a, R and T are the permeability, pre-exponential factor, activation energy, gas constant and Kelvin temperature, respectively.

In comparison with the CMSMs without ZSM-5 zeolite, the gas permeability of the CZ membrane with ZSM-5 zeolite is much lower under the same permeating conditions. The variation in the permeability of different gases differs to a great degree, resulting

Table 1
Gas separation performance of carbon membranes for single and mixed gases.

Sample code	Permeation temperature (°C)	Single gases							Mixed gas O_2/N_2 (21/79 vol. ratio)	
		Permeability (Barrer[a])				Ideal selectivity			Permeability of O_2 (Barrer)	Selectivity
		H_2	CO_2	O_2	N_2	H_2/N_2	CO_2/N_2	O_2/N_2		
CM	90	342.1	256.2	131.5	13.6	25.2	18.8	9.7	–	–
	70	320.7	229.3	97.8	12.9	24.8	17.8	7.6	–	–
	50	285.2	200.6	70.3	11.8	24.2	17.0	6.0	33.2	5.1
CZ	50	264.2	30.7	13.0	3.1	85.8	10.0	4.2	4.2	4.1
Ref. [7]	100	–	24.3	11.4	1.7	–	14	6.7	–	–
Ref. [39]	100	–	37[b]	–	2.5[b]	–	14	–	–	–
Ref. [40][c]	100	–	21.0	9.5	1.8	–	11.8	5.4	–	–

[a] 1 Barrer $=10^{-10}$ cm^3 (STP) cm/cm^2 s cmHg $=3.35\times10^{-16}$ mol m/m^2 s Pa.
[b] The permeabilities should be $\times10^{-9}$ with the unit of mol/m^2 s Pa.
[c] The permeabilities were obtained by converting the original unit mol/m^2 s Pa into Barrer with the effective membrane thickness of 5.41 μm estimated from provided SEM.

in the substantial increment of H_2/N_2 selectivity to 85.8. Similar phenomenon for gas permeability of CO_2 was also observed by adding KY type zeolite into the carbon membranes [41]. This phenomenon may be due to the compact microstructure between the interfaces of carbon and zeolite phase, and the blockage of porous passages in zeolite by amorphous carbon in the pyrolysis step [25]. It should be noted that a large percentage of the porosity in the CZ membranes is the blind (impermeable) pores due to the pore shrinkage or blockage by amorphous carbons formed in the pyrolysis step. Nevertheless, the porous structure of the ZSM-5 composite membranes can be tuned to a great degree, which gives rise to an improved selectivity.

The gas permeability for the CZ membranes can also be tuned by changing the concentration and the viscosity of membrane-forming solution in the beginning. The membrane-forming solution with smaller concentration or lower viscosity is easier to infiltrate into the porous channels of the incorporated ZSM-5, resulting in the CMSMs with improved microstructure and gas permselectivity but poor membrane integrity. The process needs to be further optimized in terms of the structure and gas separation performance of the concerned membranes.

From Table 1, it is interesting to see that the as-made CMSMs exhibit substantially high ideal selectivity for H_2/N_2, CO_2/N_2 and O_2/N_2 gas pairs, which is one order higher in comparison with the CMSMs made from Ultem 1000 PEI [7], BPDA–pp'ODA [42] and BPDA–pPDA polyimides [43].

In contrast with single gases, both lower oxygen permeability and selectivity is observed for the gas mixture of O_2/N_2 due to the competitive permeation through the CMSMs. Similar drop in permeability for gas mixtures was also found by other researchers [44].

An ideal membrane is expected to have both high permeability and high selectivity [45]. Fig. 10 shows the separation data for the O_2/N_2 mixture gas of the as-made CMSMs, which is Robeson's plot. It can be seen that most of the gas separation data of the CMSMs reported in the literature are in the region between the upper bounds of polymeric and carbon membranes. It is noteworthy that the as-made CMSMs in the present work are much better than many reported results in the literature, showing both high permeability and high selectivity, which is highly attractive for commercial applications.

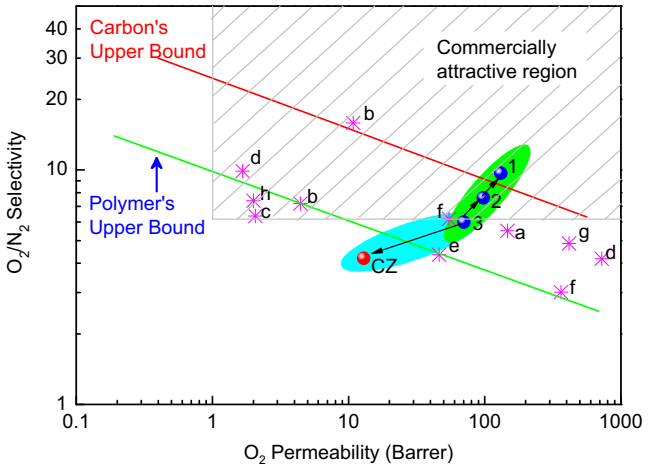

Fig. 10. Correlation of O_2 permeability with O_2/N_2 selectivity of carbon membranes made from different precursors. Notes: a. PPES [46]; b. PPESK [25]; c. phenolic resin [47]; d. poly(furfuryl alcohol) [48]; e. polyimide [49]; f. polyimide [50]; g. polyimide [51]; h. polyetherimide [7]; 1, 2, 3, CZ, ODPA–ODA type polyetherimide in this work.

4. Conclusions

Carbon membranes for gas separation have been successfully fabricated from ODPA–ODA type polyetherimide. It has been found that the preoxidation step is necessary to make defect-free carbon membranes, which helps to improve the thermal stability of the precursor and to form crosslinked structure in the membranes. The preoxidation temperature is an important factor that needs to be controlled precisely in order to tune the crosslinking reactions and to prevent the excessive oxidation of the polymer molecules. For the ODPA–ODA PEI-derived carbon membranes, the involved gas separation mechanism is a molecular sieving one. For the carbon membranes made first at 480 °C for the preoxidation and then at 650 °C for pyrolysis, the gas permeability of 342.1 Barrer for H_2, 256.2 Barrer for CO_2, 131.5 Barrer for O_2 and 13.6 Barrer for N_2, along with the ideal selectivity of 25.2 for H_2/N_2, 18.8 for CO_2/N_2 and 9.7 for O_2/N_2, have been achieved. The addition of zeolite ZSM-5 helps to significantly improve the H_2/N_2 selectivity of the carbon membranes.

Acknowledgments

This work was partly supported by the National Natural Science Foundation of China (No. 20906063), the Liaoning Natural Science Foundation of China (20102170), the Program for Liaoning Excellent Talents in University (LJQ2012010), and the State Key Laboratory of Fine Chemicals (KF1107). The authors would like to thank Mr. Hao Wu and Dr. Junhua You for their help in Elemental and XRD analysis, and Prof. Michael D. Guiver for help in polishing the English.

References

[1] R. Singh, W.J. Koros, Carbon molecular sieve membrane performance tuning by dual temperature secondary oxygen doping (DTSOD), J. Membr. Sci. 427 (2013) 472–478.
[2] A.F. Ismail, D. Rana, T. Matsuura, H.C. Foley, Carbon-Based Membranes for Separation Processes, Springer, New York, 2011.
[3] S.H. Han, G.W. Kim, C.H. Jung, Y.M. Lee, Control of pore characteristics in carbon molecular sieve membranes (CMSM) using organic/inorganic hybrid materials, Desalination 233 (2008) 88–95.
[4] Y.H. Sim, H. Wang, F.Y. Li, M.L. Chua, T.S. Chung, M. Toriida, S. Tamai, High performance carbon molecular sieve membranes derived from hyperbranched polyimide precursors for improved gas separation applications, Carbon 53 (2013) 101–111.
[5] S.S. Hosseini, M.R. Omidkhah, A.Z. Moghaddam, V. Pirouzfar, W.B. Krantz N.R. Tan, Enhancing the properties and gas separation performance of PBI–polyimides blend carbon molecular sieve membranes via optimization of the pyrolysis process, Sep. Purif. Technol. 122 (2014) 278–289.
[6] W.N.W. Salleh, A.F. Ismail, T. Matsuura, M.S. Abdullah, Precursor selection and process conditions in the preparation of carbon membrane for gas separation: a review, Sep. Purif. Rev. 40 (2011) 261–311.
[7] A.B. Fuertes, T.A. Centeno, Carbon molecular sieve membranes from polyetherimide, Microporous Mesoporous Mater. 26 (1998) 23–26.
[8] M.G. Sedigh, L. Xu, T.T. Tsotsis, M. Sahimi, Transport and morphological characteristics of polyetherimide-based carbon molecular sieve membranes, Ind. Eng. Chem. Res. 38 (1999) 3367–3380.
[9] M.G. Sedigh, M. Jahangiri, P.K.T. Liu, M. Sahimi, T.T. Tsotsis, Structural characterization of polyetherimide-based carbon molecular sieve membranes, AIChE J. 46 (2000) 2245–2255.
[10] E.P. Favvas, E.P. Kouvelos, G.E. Romanos, G.I. Pilatos, A.Ch. Mitropoulos N.K. Kanellopoulos, Characterization of highly selective microporous carbon hollow fiber membranes prepared from a commercial co-polyimide precursor, J. Porous Mater. 15 (2008) 625–633.
[11] E. Barbosa-Coutinho, V.M.M. Salim, C.P. Borges, Preparation of carbon hollow fiber membranes by pyrolysis of polyetherimide, Carbon 41 (2003) 1707–1714.
[12] A.K. Gupta, D.K. Paliwal, P. Bajaj, Acrylic precursors for carbon fibers, J. Macromol. Sci.-Polym. Rev. 31 (1991) 1–89.
[13] B. Zhang, T. Wang, S. Liu, S. Zhang, J. Qiu, Z. Chen, H. Cheng, Structure and morphology of microporous carbon membrane materials derived from poly (phthalazinone ether sulfone ketone), Microporous Mesoporous Mater. 96 (2006) 79–83.
[14] S.S. Hosseini, T.S. Chung, Carbon membranes from blends of PBI and polyimides for N_2/CH_4 and CO_2/CH_4 separation and hydrogen purification, J. Membr. Sci. 328 (2009) 174–185.
[15] W.N.W. Salleh, A.F. Ismail, Carbon hollow fiber membranes derived from PEI/PVP for gas separation, Sep. Purif. Technol. 80 (2011) 541–548.
[16] W.N.W. Salleh, A.F. Ismail, Fabrication and characterization of PEI/PVP-based carbon hollow fiber membranes for CO_2/CH_4 and CO_2/N_2 separation, AIChE J. 58 (2012) 3167–3175.
[17] M.Y. Wey, H.H. Tseng, C.K. Chiang, Effect of MFI zeolite intermediate layers on gas separation performance of carbon molecular sieve (CMS) membranes, J. Membr. Sci. 446 (2013) 220–229.
[18] R. Varun, A. Amba, R. Young, J.E. McGrath, L.W. Garth, Thermal stability, crystallization kinetics and morphology of a new semi crystalline polyimide based on 1,3-bis(4-amino-phenoxy) benzene and 3,3′,4,4′-biphenyltetracarboxylic dianhydride, Polymer 41 (2000) 8121–8138.
[19] M. Kulkarni, S. Kothawade, G. Arabale, D. Wagh, K. Vijayamohanan R.A. Kulkarni, S.P. Vernekar, Synthesis and characterization of polyimides and co-polyimides having pendant benzoic acid moiety, Polymer 46 (2005) 3669–3676.
[20] Y. Xu, C. Chen, P. Zhang, B. Sun, J. Li, Pervaporation properties of polyimide membranes for separation of ethanol+water mixtures, J. Chem. Eng. Data 51 (2006) 1841–1845.
[21] S. Neyertz, D. Brown, Molecular dynamics simulations of oxygen transport through a fully atomistic polyimide membrane, Macromolecules 41 (2008) 2711–2721.
[22] S. Neyertz, A. Douanne, D. Brown, A molecular dynamics simulation study of surface effects on gas permeation in free-standing polyimide membranes, J. Membr. Sci. 280 (2006) 517–529.
[23] J.H. Shim, L.Y. Jung, S.W. Pyo, Y.K. Kim, Organic thin-film transistors with ODPA–ODA polyimide as a gate insulator through vapor deposition polymerization, Thin Solid Films 441 (2003) 284–286.
[24] Q. Liu, T. Wang, C. Liang, B. Zhang, S. Liu, Y. Cao, J. Qiu, Zeolite married to carbon: a new family of membrane materials with excellent gas separation performance, Chem. Mater. 18 (2006) 6283–6288.
[25] B. Zhang, T. Wang, Y. Wu, Q. Liu, S. Liu, Z. Zhang, J. Qiu, Preparation and gas permeation of composite carbon membranes from poly(phthalazinone ether sulfone ketone), Sep. Purif. Technol. 60 (2008) 259–263.
[26] B. Zhang, Y. Shi, Y. Wu, T. Wang, J. Qiu, Towards the preparation of ordered mesoporous carbon/carbon composite membranes for gas separation, Sep. Sci. Technol. 49 (2014) 171–178.
[27] W.N.W. Salleh, A.F. Ismail, Effect of stabilization temperature on gas permeation properties of carbon hollow fiber membrane, J. Appl. Polym. Sci. 127 (2013) 2840–2846.
[28] W.N.W. Salleh, A.F. Ismail, Effect of stabilization condition on PEI/PVP-based carbon hollow fiber membranes properties, Sep. Sci. Technol. 48 (2013) 1030–1039.
[29] S.I. Kuroda, I. Mita, Degradation of aromatic polymers-II. The crosslinking during thermal and thermo-oxidative degradation of a polyimide, Eur. Polym. J. 25 (1989) 611–620.
[30] D.W. Wallace, J. Williams, C. Staudt-Bickel, W.J. Koros, Characterization of crosslinked hollow fiber membranes, Polymer 47 (2006) 1207–1216.
[31] Y. Xiao, T.S. Chung, H.M. Guan, M.D. Guiver, Synthesis, cross-linking and carbonization of co-polyimides containing internal acetylene units for gas separation, J. Membr. Sci. 302 (2007) 254–264.
[32] A.B. Fuertes, Effect of air oxidation on gas separation properties of adsorption-selective carbon membranes, Carbon 39 (2001) 697–706.
[33] S.T. Amancio-Filho, J. Roeder, S.P. Nunes, J.F. dos Santos, F. Beckmann, Thermal degradation of polyetherimide joined by friction riveting (fricriveting), part I: influence of rotation speed, Polym. Degrad. Stab. 93 (2008) 1529–1538.
[34] K. Vanherck, G. Koeckelberghs, I.F.J. Vankelecom, Crosslinking polyimides for membrane applications: a review, Prog. Polym. Sci. 38 (2013) 874–896.
[35] A.S. Gabriel, E. Irena, S. Moshe, Carbon membranes for high temperature gas separations: experiment and theory, AIChE J. 50 (2004) 596–610.
[36] M.B. Saeed, M.S. Zhan, Effects of monomer structure and imidization degree on mechanical properties and viscoelastic behavior of thermoplastic polyimide films, Eur. Polym. J. 42 (2006) 1844–1854.
[37] E.L. Wu, S.L. Lawton, D.H. Olson, A.C. Rohrman, G.T. Kokotailo, ZSM-5-type materials. Factors affecting crystal symmetry, J. Phys. Chem. 83 (1979) 2777–2781.
[38] Q. Liu, T. Wang, J. Qiu, Y. Cao, A novel carbon/ZSM-5 nanoeomposite membrane with high performance for oxygen/nitrogen separation, Chem. Commun. 42 (2006) 1230–1232.
[39] T.A. Centeno, A.B. Fuertes, Supported carbon molecular sieve membranes based on phenolic resin, J. Membr. Sci. 160 (1999) 201–211.
[40] M. Yoshimune, K. Mizoguchi, K. Haraya, Alcohol dehydration by pervaporation using a carbon hollow fiber membrane derived from sulfonated poly(phenylene oxide), J. Membr. Sci. 425–426 (2013) 149–155.
[41] P.S. Tin, T.S. Chung, L. Jiang, S. Kulprathipanja, Carbon–zeolite composite membranes for gas separation, Carbon 43 (2005) 2013–2032.
[42] K. Kusakabe, M. Yamamoto, S. Morooka, Gas permeation and micropore structure of carbon molecular sieving membranes modified by oxidation, J. Membr. Sci. 149 (1998) 59–67.
[43] A.B. Fuertes, T.A. Centeno, Preparation of supported carbon molecular sieve membrane, Carbon 37 (1999) 679–684.
[44] A. Singh-Ghosal, W.J. Koros, Air separation properties of flat sheet homogeneous pyrolytic carbon membranes, J. Membr. Sci. 174 (2000) 177–188.
[45] L.M. Robeson, The upper bound revisited, J. Membr. Sci. 320 (2008) 390–400.
[46] B. Zhang, G. Shen, Y. Wu, T. Wang, J. Qiu, T. Xu, C. Fu, Preparation and characterization of carbon membranes derived from poly(phthalazinone ether sulfone) for gas separation, Ind. Eng. Chem. Res. 48 (2009) 2886–2890.
[47] H. Kita, H. Maeda, K. Tanaka, K.-i. Okamoto, Carbon molecular sieve membrane prepared from phenolic resin, Chem. Lett. 26 (1997) 179–180.
[48] M.B. Shiflett, H.C. Foley, On the preparation of supported nanoporous carbon membranes, J. Membr. Sci. 179 (2000) 275–282.
[49] A.B. Fuertes, D.M. Nevskaia, T.A. Centeno, Carbon composite membranes from Matrimid® and Kapton® polyimides for gas separation, Microporous Mesoporous Mater. 33 (1999) 115–125.
[50] K. Haraya, H. Suda, H. Yanagishita, S. Matsuda, Asymmetric capillary membrane of a carbon molecular sieve, Chem. Commun. (1995) 1781–1782.
[51] K. Okamoto, S. Kawamura, M. Yoshino, H. Kita, Olefin/paraffin separation through carbonized membranes derived from an asymmetric polyimide hollow fiber membrane, Ind. Eng. Chem. Res. 38 (1999) 4424–4432.